Hydrodynamics at RHIC – how well does it work, where and how does it break down?

Ulrich Heinz†§

† Physics Department, The Ohio State University, Columbus, OH 43210

Abstract. I review the successes and limitations of the ideal fluid dynamic model in describing hadron emission spectra from Au+Au collisions at the Relativistic Heavy Ion Collider (RHIC).

1. Introduction

For the last 6-8 months, an intense discussion has been going on in the relativistic heavy-ion collision (RHIC) community whether one can consider the discovery of the quark-gluon plasma (QGP) as settled and if it is time for the RHIC program to move on, entering a new phase of detailed and precise measurements to explore the quantitative properties of this new state of hot and dense matter [1, 2]. Whereas theorists seem to generally agree that QGP has been successfully created in Au+Au collisions at RHIC [1, 3], the experimental collaborations are more cautious in their assessments [2]. General agreement exists, however, that RHIC has produced thermalized matter at unprecedented high energy density. This conclusion is based on the successful hydrodynamic description of the measured hadron momentum spectra, in particular the elliptic flow and its "fine structure", i.e. its dependence on the hadron mass [4].

Hydrodynamics provides a direct link between the equation of state (EOS) of the expanding fluid and the flow pattern manifested in the emitted hadron spectra. Just like any other phase transition, the quark-hadron phase transition in QCD generates a "soft" region in the EOS within which the ability of the pressure to generate flow is greatly reduced. This is expected to leave visible traces in the *flow excitation function*. For example, hydrodynamics predicts that the elliptic flow coefficient v_2 should show a non-monotonic dependence on the collision energy [5], arising from a reduction in the elliptic flow signal if the collision fireball spends the crucial early stage, where such flow would be created, in the phase transition region.

A quantitative determination of the EOS requires precision flow data as well as systematic theoretical studies of the influence of the initial conditions, equation of state, non-ideal transport effects, and the final decoupling kinetics on the observed hadron spectra. With the present theory and RHIC data, we are just at the beginning of such a program. That the RHIC data so far provide strong support for the basic validity of the hydrodynamic approach is a good omen, raising the hope that such quantitative studies will be ultimately successful. There would be much less optimism if RHIC had repeated the history of lower-energy heavy-ion collisions where

§ email: heinz@mps.ohio-state.edu. Work supported by the U.S. Department of Energy under Grant No. DE-FG02-01ER41190

hydrodynamics never worked well enough to provide more than a rough qualitative understanding of the collision dynamics. When the fireball dynamics proceeds too far away from local thermal equilibrium, it requires a microscopic transport theoretical description, involving a variety of non-equilibrium mechanisms with typically poorly constrained parameters. This renders the extraction of the equation of state difficult and uncertain.

Of course, even at RHIC the hydrodynamic approach has its limitations. Ideal fluid dynamics, which assumes instantaneous local thermal equilibration, always remains an idealization; however, quantitative control of possibly small non-ideal effects due to shear and bulk viscosity, heat conduction and diffusion requires a numerical implementation of *viscous relativistic hydrodynamics* which has its technical and conceptual difficulties and is only now beginning to become practical [6]. Furthermore, in very peripheral heavy-ion collisions, where the size and lifetime of the collision fireball become small, even a viscous hydrodynamic approach is expected to eventually break down. Also, particles with very large transverse momenta (jets) are never expected to suffer sufficiently many interactions with the fireball medium to fully thermalize before escaping; hence a hydrodynamic approach can never work at very high $p_\perp$. However, we can turn this inescapable failure of hydrodynamics in small collision systems and at high $p_\perp$ to our favor: since ideal fluid dynamics appears to work well in near-central collisions, near mid-rapidity, and at low $p_\perp \lesssim 1.5 - 2\,\mathrm{GeV}/c$ [4], we can study its gradual breakdown at larger impact parameters, rapidities, and transverse momenta in order to learn something about the mechanisms for the *approach to thermal equilibrium* at the beginning of the collision and the *decay of thermal equilibrium* near the end of the expansion stage, and hence about the transport properties of the early quark-gluon plasma and the late hadron resonance gas created in these collisions. In this talk I will lay out the beginnings of such a program.

2. Hydrodynamic description of single particle spectra and elliptic flow

If the dense matter formed in the nuclear collision thermalizes locally on a time scale much shorter than any macroscopic dynamical scale, its evolution can be described by ideal fluid dynamics. The fluid's state is then completely determined by the space-time profiles for its energy density $e(x)$, baryon density $n(x)$, and flow 4-velocity $u^\mu(x)$. The equation of state $p(e, n)$ closes the set of equations. Small deviations from local thermal equilibrium result in viscous corrections to the ideal fluid decomposition of energy-momentum tensor and baryon current, involving gradients of the above profiles multiplied by transport coefficients. For large deviations from local thermal equilibrium this expansion in terms of gradients of e, n and u^μ breaks down, and the macroscopic hydrodynamic approach must be replaced by a microscopic kinetic one which evolves the distribution functions in both coordinate and momentum space.

Ideal fluid dynamics does not work during the initial collision stage, when the two colliding nuclei penetrate each other, converting some of their initial kinetic energy into creation of new matter, and it is also inapplicable during the last stage of the collision when the expanding matter becomes so dilute that interactions among its constituents are rare and local equilibrium breaks down. The hydrodynamic model therefore needs *initial conditions* (supposedly the result of an early pre-equilibrium quantum kinetic evolution leading to initial thermalization) and *final conditions* (a freeze-out criterium describing the transition from a locally thermalized fluid to an ensemble of free-streaming, noninteracting hadrons). Both initial and final conditions

involve free parameters which must be tuned to data. As described in some detail in [7], they can all be fixed by only using data on the collision centrality dependence of the charged particle multiplicity and the *pion* and *proton* transverse momentum spectra in *central* ($b = 0$) collisions. All other hadron spectra from central collisions, and all features of all hadron spectra in non-central collisions (in particular the elliptic flow for all hadron species) are then parameter-free predictions of the model [8].

For 130 A GeV and 200 A GeV Au+Au collisions at RHIC, these predictions were surprisingly successful (see review in [4]). Figure 1 shows the fit to the (absolutely normalized) pion and antiproton spectra and, as examples, the predictions for the

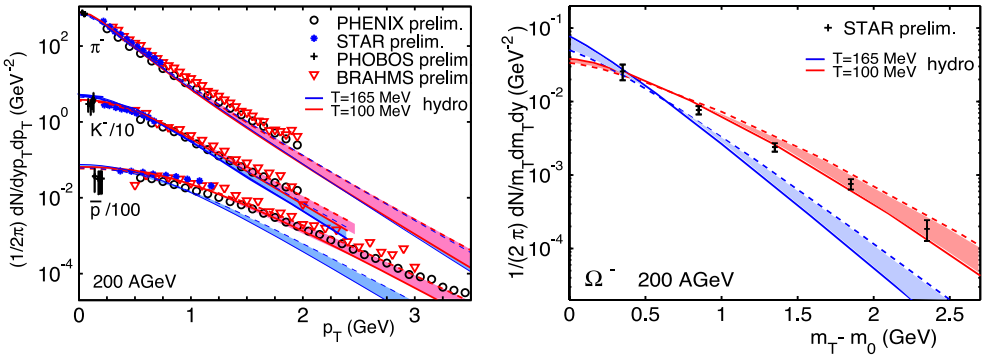

Figure 1. (Color online) Negative pion, kaon, antiproton, and Ω spectra from central Au+Au collisions at $\sqrt{s} = 200\,A$ GeV, as measured by the four RHIC experiments [9, 10, 11, 12, 13]. The curves show hydrodynamical calculations [14, 4] as described in the text.

kaon and Ω spectra from 200 A GeV Au+Au collisions. Two sets of theoretical curves [14] are shown: the lower (blue) bands correspond to kinetic decoupling directly after hadronization at $T_{\rm cr} = 165$ MeV, whereas the upper (red) bands assume decoupling at $T_{\rm dec} = 100$ MeV. The width of the bands indicates the sensitivity of the calculated spectra to an initial transverse flow of the fireball already at the time of thermalization (for details see [14]). The hydrodynamic model output shows [5] that it takes about 9-10 fm/c until the fireball has become sufficiently dilute to completely convert to hadronic matter, and another 7-8 fm/c to completely decouple. Figure 1 shows clearly that by the time of hadronization hydrodynamics has not yet generated enough radial flow to reproduce the measured $\bar{p}$ and Ω spectra; these heavy hadrons, which are particularly sensitive to radial flow effects, require the additional collective "push" created by resonant (quasi)elastic interactions during the fairly long-lived hadronic rescattering stage between $T_{\rm cr}$ and $T_{\rm dec}$. The late hadronic stage of the collision thus plays an important role for the quantitative understanding of the shape of the single particle spectra at RHIC and their radial flow.

This is different for the elliptic flow which is driven by the spatial anisotropy of the reaction zone in non-central collisions and the resulting anisotropic pressure gradients: as shown in [5], at RHIC energies, for not too peripheral Au+Au collisions, the momentum anisotropy *saturates before the completion of hadronization*, due to the disappearance of the spatial deformation of the fireball. The measured v_2 thus reflects almost exclusively the early QGP dynamics and the phase transition region. Figure 2 shows that the corresponding hydrodynamic predictions work very well, at least for transverse momenta below about 1.5-2 GeV/c where most ($> 99\%$) of the particles

are emitted.

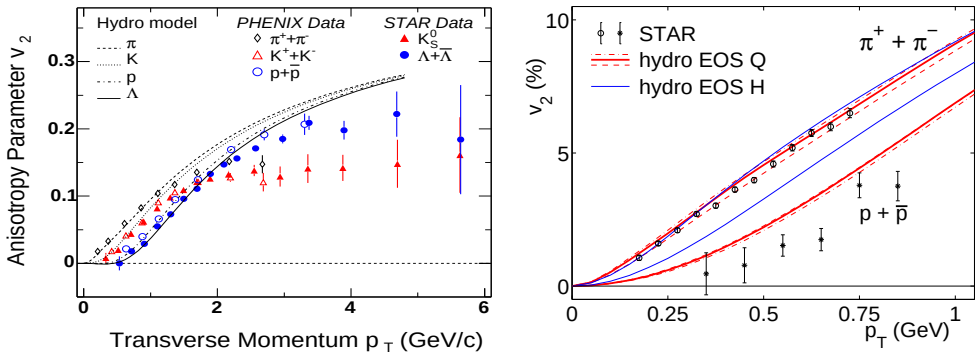

Figure 2. (Color online) Differential elliptic flow $v_2(p_\perp)$ for several identified hadron species from minimum bias Au+Au collisions at 130 (right [16]) and 200 A GeV (left [15]), compared with hydrodynamic predictions [8].

Hydrodynamics predicts a characteristic rest mass dependence of v_2 [8] which is nicely reproduced by the data in Fig. 2. This "fine structure" constitutes compelling evidence that the hot matter produced at RHIC behaves like a thermalized fluid. The "mass scaling" of v_2 seen at low $p_\perp$ is quite distinct from the "quark number scaling" of v_2 seen at larger transverse momenta $p_\perp \gtrsim 2-4\,\mathrm{GeV}/c$ [15]; the latter is characteristic of a quark-coalescence mechanism for hadron production which dominates in that $p_\perp$ range [17]. The mass scaling seen in the hydrodynamic regime is sensitive to the EOS of the fireball matter: the right panel in Fig. 2 shows two calculations, one without a phase transition (EOS H), the other including the quark-hadron transition (EOS Q). Although neither one fits the STAR proton data particularly well, the latter show a clear preference for the EOS including a phase transition.

3. Where ideal hydrodynamics breaks down

The elliptic flow coefficient $v_2(p_\perp)$ is a measure for the (relatively small) differences between the transverse momentum spectra with momenta pointing into and perpendicular to the reaction plane. As such, it is more sensitive to deviations from ideal hydrodynamic behaviour than the overall shapes (slope parameters) of the transverse momentum spectra. Two model studies [18, 19] showed that v_2 reacts particularly strongly to shear viscosity. As the mean free path of the plasma constituents (and thus the fluid's viscosity) goes to zero, v_2 approaches the ideal hydrodynamic limit from below [20, 21] (see Fig. 3a). At higher transverse momenta it does so more slowly than at low $p_\perp$ [21], approaching a constant saturation value as seen in the data rather than following the hydrodynamic almost linear rise as a function of $p_\perp$ shown by the lines in Fig. 2. The increasing deviation from the ideal fluid limit for growing $p_\perp$ is qualitatively consistent with the expected influence of shear viscosity: Teaney [19] showed that viscous corrections to the local thermal equilibrium distribution function increase in first order quadratically with $p_\perp$, leading to stronger and stronger reduction of v_2 below the ideal fluid limit as $p_\perp$ grows (see Fig. 3b). From the results in Fig. 3b Teaney concluded that at RHIC the normalized sound attenuation length $\frac{\Gamma_s}{\tau} = \frac{4}{3T\tau}\frac{\eta}{s}$ (where η is the shear viscosity, T the temperature and s the entropy

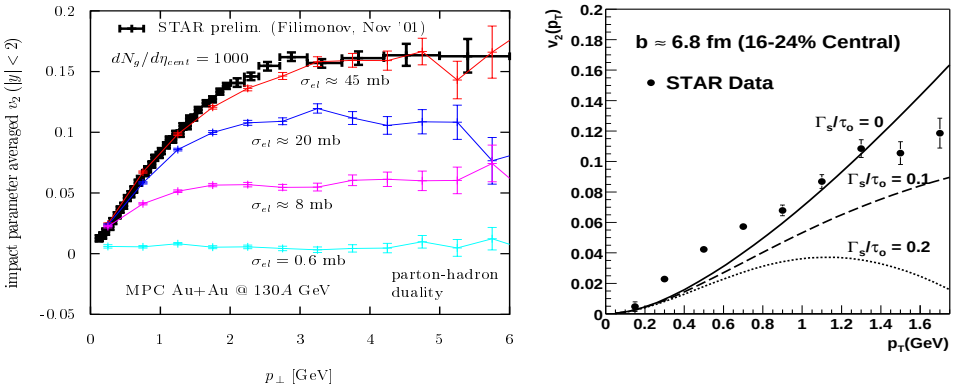

Figure 3. (Color online) Left: Elliptic flow from a parton cascade [21], compared with STAR data, for different parton-parton scattering cross sections. Larger cross sections lead to smaller mean free paths. Right: Perturbative effects of shear viscosity on the elliptic flow $v_2(p_\perp)$ [19] (see text for discussion).

density) cannot be much larger than about 0.1. This puts a stringent limit on the dimensionless ratio η/s, bringing it close to the recently conjectured absolute lower limit for the viscosity of $\eta/s = \hbar/(4\pi)$ [22]. This would make the quark-gluon plasma the most ideal fluid ever observed [22].

These arguments show that deviations from ideal fluid dynamics at high $p_\perp$ must be expected, and that they can be large even for fluids with very low viscosity. At which $p_\perp$ non-ideal effects begin to become visible in $v_2(p_\perp)$ can be taken as a measure for the fluid's viscosity. Figure 2a, however, shows that mesons seem to deviate from the ideal fluid dynamical prediction earlier than baryons which follow the hydrodynamic curves to considerably larger $p_\perp$, thereby reaching significantly larger saturation values for v_2. Why should viscous effects be different for baryons and mesons? In fact, both the $p_\perp$-value where v_2 begins to drop below the hydrodynamic prediction and the asymptotic saturation values of v_2 appear to be independent of the hadron mass and only care about whether the hadron is a meson or a baryon!

This "valence quark number scaling" of v_2 at intermediate and high $p_\perp$ can be explained through quark coalescence [17]. This model predicts that the elliptic flow divided by the number of valence quarks n, plotted against $p_\perp/n$, should be a universal function which reflects the partonic collective elliptic flow just before hadronization: $v_2^{\rm part}(p_\perp) = \frac{v_2^{\rm had}}{n}\left(\frac{p_\perp^{\rm had}}{n}\right)$ [17]. For $p_\perp \gtrsim 750\,$MeV, this scaling works extremely well [15], at *all collision centralities* (note that v_2 is a strong function of centrality!). Strange and non-strange partons seem to carry the same elliptic flow [15], consistent with strong rescattering and thermalization in the partonic phase. Below $p_\perp \sim 750\,$MeV the extracted partonic elliptic flow follows the hydrodynamically predicted almost linear rise with $p_\perp$, and quark number scaling is violated and replaced by the hydrodynamically predicted mass scaling. In summary, the critical value of $p_\perp$ where QGP viscosity manifests itself in the partonic elliptic flow is $\approx 750\,$MeV$/c$. What this implies for the value of the QGP shear viscosity η remains to be seen, by comparing the data to simulations with a viscous relativistic hydrodynamic code.

Hydrodynamics also fails to describe the elliptic flow v_2 in more peripheral Au+Au collisions at RHIC, in central and peripheral collisions at lower energies (for both see Fig. 4a), and in minimum bias collisions at RHIC at forward rapidities [25]. Whereas hydrodynamics predicts a non-monotonic beam energy dependence of v_2 [5], with largest values at upper AGS and lower SPS energies (see Fig. 4a), somewhat lower values at RHIC and again larger values at the LHC, the data seem to increase monotonically with $\sqrt{s}$.

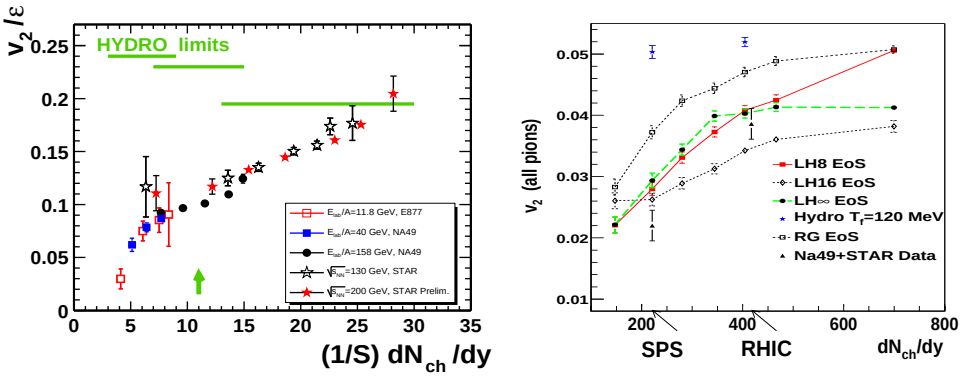

Figure 4. (Color online) Left: Scaled elliptic flow v_2/ϵ (where ϵ denotes the initial spatial eccentricity) vs. the charged multiplicity density per unit initial transverse overlap area S [23]. Right: Elliptic flow v_2 for minimum bias Au+Au collisions at various collision energies, parametrized by the final charged multiplicity density at midrapidity [24]. See text for discussion.

Such a monotonic rise is consistent with "hybrid" calculations by Teaney [24] (Fig. 4b) where the fireball undergoes ideal fluid dynamic evolution only to a point just below the hadronization phase transition, followed by hadronic *kinetic* evolution using the RQMD code until final decoupling. Figure 4b shows several curves corresponding to different equations of state during the hydrodynamic evolution (see [24] for details), with LH8 being closest to the data. The difference between the points labelled LH8 and the hydrodynamic values at the top of the figure is due to the different evolution during the late hadronic stage. Obviously, at lower collision energies and for impact parameters $b \sim 7$ fm (which dominate v_2 in minimum bias collisions), ideal fluid dynamics continues to build additional elliptic flow during the hadronic stage, in contrast to RQMD. The reason for the additional hadronic v_2 in the hydrodynamic simulations is that at lower beam energies the initial energy densities are smaller and the fireball does not spend enough time in the QGP phase for the spatial eccentricity ϵ to fully disappear before entering the hadron resonance gas phase. Anisotropic pressure gradients thus still exist in the hadronic phase, and hydrodynamics reacts to them according to the stiffness of the hadron resonance gas EOS ($p \approx 0.15e$). Teaney's calculations [24] show that RQMD reacts to these remaining anisotropies much more weakly, building very little if anny additional elliptic flow during the hadronic phase. The hadron resonance gas, as modelled in RQMD, is a highly viscous medium, unable to reach or maintain local thermal equilibrium and therefore not behaving as an ideal fluid at all. The failure of the hydrodynamic model in peripheral collisions at RHIC and in central and peripheral collisions at the SPS and AGS is therefore *not* necessarily caused by the absence of an ideal fluid QGP phase during the early expansion stage,

but rather by the highly viscous late hadronic stage which is unable to efficiently react to the remaining spatial fireball eccentricity. Similar arguments hold at forward rapidities at RHIC [26] where the initial energy densities are also significantly smaller than at midrapidity while the initial spatial eccentricities are similar.

The large hadron gas viscosity spoils one of the clearest experimental signatures for the existence of the quark-hadron phase transition, the predicted non-monotonic beam energy dependence of v_2 [5]. The ideal fluid dynamic limit for v_2 scales with the speed of sound $c_s^2 = \frac{\partial p}{\partial e}$. As one passes from the hadron resonance gas through the phase transition into the QGP, c_s^2 varies from about 0.15 in the hadron gas to about $\frac{1}{3}$ in the QGP, going through a minimum near zero in the soft transition region. Ideal fluid dynamics maps this behaviour directly onto v_2 as one changes the initial energy density by increasing the collision energy. As one comes down from infinite beam energy, v_2 is therefore predicted to first decrease (due to the softening of the EOS in the phase transition region) and then recover somewhat in the moderately stiff hadron gas phase. The hadron gas viscosity spoils this recovery, leading to an apparently monotonous decrease of v_2 with falling beam energy (Fig. 4). However, recent PHENIX data from Au+Au collisions at $\sqrt{s} = 62\,A\,\mathrm{GeV}$ [27] indicate that this decrease may not be quite as monotonous as suggested by Fig. 4a. They show essentially constant elliptic flow over the entire energy range explored at RHIC (from 62 to 200 A GeV), decreasing only when going further down to SPS and AGS energies. While this is does not confirm the hydrodynamically predicted *rise* of v_2, it may still be a strongly diluted reflection of this predicted non-monotonic structure in the elliptic flow excitation function. Obviously, many and more systematic hybrid calculations of the type pioneered by Teaney [24] are necessary to explore to what extent we can eventually prove the existence of a QCD phase transition using elliptic flow data.

We recently pointed out [28] a very nice possibility to extend Fig. 4a towards the right, in order to confirm that for higher initial energy densities the measured v_2 indeed settles on the ideal hydrodynamic curve. By colliding deformed uranium nuclei at RHIC, using the Zero Degree Calorimeters to select only full overlap collisions, and then exploiting the known binary collision component in the produced charged particle multiplicity to select configurations with different initial spatial eccentricities by cutting on multiplicity, one can extend the explored region in Fig. 4a by about 60% along the horizontal axis. In fact, the lowest value for $\frac{1}{S}\frac{dN_{\mathrm{ch}}}{dy}$ obtainable in this way is for U+U collisions in the side-on-side configuration, which reproduce similar initial energy densities as central Au+Au collisions, but with a large initial eccentricity of 25%. The opposite limit is reached for U+U collisions in the nose-on-nose configuration where the elliptic flow approaches zero but $\frac{1}{S}\frac{dN_{\mathrm{ch}}}{dy}$ is about 60% higher than the largest value plotted in Fig. 4a.

4. Conclusions

The excellent reproduction of all aspects of single-particle hadron spectra measured in central and semicentral Au+Au collisions at RHIC, including the elliptic flow and its fine structure, by relativistic hydrodynamics provides strong evidence for the creation of a thermalized medium at high energy density $e > 10\,\mathrm{GeV/fm}^3$ with thermalization time $\tau_{\mathrm{therm}} < 1\,\mathrm{fm}/c$. The only known thermalized state at such energy densities it the quark-gluon plasma. The observation of quark-number scaling of the elliptic flow and other observables at intermediate $p_\perp$ indicates that deconfined valence quarks play a dynamical role in hadron production, providing at least indirect evidence for color

deconfinement. The almost ideal fluid behaviour of the expanding fireball shows that the QGP is a strongly coupled plasma with fluid-like rather than gas-like properties and with the lowest viscosity of any known liquid. In contrast to the QGP, the hadron gas dominating the late expansion stage is highly viscous and does not behave like an ideal fluid. Hydrodynamics works for the first time quantitatively at RHIC since the fireball dynamics is for the first time dominated by the QGP.

We have reached an interesting stage where we are beginning to explore the detailed properties of this new QGP state of matter. Clearly, many detailed studies, both theoretical and experimental, are required to achieve that goal. Systematic hydrodynamic studies, combined with high statistics data on spectra and elliptic flow, should help to further constrain the thermalization time $\tau_{\rm therm}$ and equation of state. Hybrid hydro+cascade calculations should be performed to isolate the non-ideal effects from the late hadronic stage. A 3+1-dimensional relativistic viscous hydrodynamic code must be developed to quantitatively constrain the transport properties of the QGP (such as its viscosity) from the data, and thereby provide phenomenological constraints for theoretical efforts to calculate the latter from first principles.

References

[1] See articles by Gyulassy M and McLerran L, Shuryak E V, Müller B, Wang X N, Stöcker H, and Blaizot J P and Gelis F 2004 in: *New Discoveries at RHIC – The Strongly Interacting QGP* (RBRC Scientific Articles, Vol. 9, Brookhaven National Laboratory, Upton, NY, USA), to appear as a special volume in *Nucl. Phys.* A.

[2] The white papers from the experimental collaborations at RHIC can be downloaded at http://www.phenix.bnl.gov/WWW/info/comment.

[3] Heinz U and Kolb P F 2002 *Nucl. Phys.* A **702** 269; Heinz U 2003 *Nucl. Phys.* A **721** 30.

[4] Kolb P F and Heinz U 2003 in: *Quark-Gluon Plasma 3*, edited by R. C. Hwa and X.-N. Wang (Singapore: World Scientific) p. 634.

[5] Kolb P F, Sollfrank J and Heinz U 2000 *Phys. Rev.* C **62** 054909.

[6] Muronga A 2004 *Phys. Rev.* C **69** 034903; Muronga A and Rischke D H 2004 *Preprint* nucl-th/0407114.

[7] Heinz U 2004 *AIP Conf. Proc.* **739** 163 [nucl-th/0407067].

[8] Huovinen P, Kolb P F, Heinz U, Ruuskanen P V and Voloshin S A 2001 *Phys. Lett.* B **503** 58.

[9] Chujo T *et al.* (PHENIX Collab.) 2003 *Nucl. Phys.* A **715** 151c.

[10] Barannikova O, Wang F, *et al.* (STAR Collab.) 2003 *Nucl. Phys.* A **715** 458c.

[11] Wosiek B *et al.* (PHOBOS Collab.) 2003 *Nucl. Phys.* A **715** 510c.

[12] Ouerdane D *et al.* (BRAHMS Collab.) 2003 *Nucl. Phys.* A **715** 478c.

[13] Suire C *et al.* (STAR Collab.) 2003 *Nucl. Phys.* A **715** 470c.

[14] Kolb P F and Rapp R 2003 *Phys. Rev.* C **67** 044903.

[15] Sorensen P R 2003 Ph.D. thesis, *Preprint* nucl-ex/0309003; Adams J *et al.* (STAR Collab.) 2004 *Phys. Rev. Lett.* **92** 052302; Adler S S *et al.* (PHENIX Collab.) 2003 *Phys. Rev. Lett.* **91** 182301.

[16] Adler C *et al.* (STAR Collab.) 2001 *Phys. Rev. Lett.* **87** 182301.

[17] Greco V, Ko C M, and Lévai P 2003 *Phys. Rev. Lett.* **90** 202302 and *Phys. Rev.* C **68** 034904; Fries R J, Müller B, Nonaka C, and Bass S A 2003 *Phys. Rev. Lett.* **90** 202303 and *Phys. Rev.* C **68** 044902; Molnar D and Voloshin S A 2003 *Phys. Rev. Lett.* **91** 092301.

[18] Heinz U and Wong S M H 2002 *Phys. Rev.* C **66** 014907.

[19] Teaney D 2003 *Phys. Rev.* C **68** 034913. communication.

[20] Zhang B, Gyulassy M and Ko C M 1999 *Phys. Lett.* B **455** 45.

[21] Molnar D and Gyulassy M 2002 *Nucl. Phys.* A **697** 495 (Erratum *ibid.* **703** 893).

[22] Kovtun P, Son D T, and Starinets A O 2004 *Preprint* hep-th/0405231.

[23] Alt C *et al.* (NA49 Collab.) 2003 *Phys. Rev.* C **68** 034903.

[24] Teaney D, Lauret J, and Shuryak E V 2001 *Preprint* nucl-th/0110037.

[25] Hirano T 2002 *Phys. Rev.* C **65** 011901.

[26] Heinz U and Kolb P F 2004 *J. Phys.* G: Nucl. Part. Phys. **30** S1229.

[27] Adler S S *et al.* (PHENIX Collab.) 2004 *Preprint* nucl-ex/0411040.

[28] Heinz U and Kuhlman A 2004 *Preprint* nucl-th/0411054.